AIAA JOURNAL
Vol. 38, No. 1, January 2000

Two Interacting Vortex Ring Pairs and Their Sound Generation

N. W. M. Ko,* R. C. K. Leung,† and K. K. Lam‡
University of Hong Kong, Hong Kong, People's Republic of China

This paper reports a numerical study of the interactions of two coaxial thin vortex ring pairs and their far-field sound generation. Out of the different varieties of widely differing near-field vortex patterns, four basic types of interactions with their associated different degrees of amplification and attenuation of the far-field sound are identified. These four types are found to depend on the circulation ratio, radius ratio, separation ratio, and phase. The suppression of the interaction, caused by the introduction of the control vortex ring pair, results in the slight and moderate attenuation of sound. The initial and continuous rapid and intense interactions with either vortex rings of the control pair are responsible for the moderate amplification and intense amplification, respectively. This study, thus, establishes the importance of the understanding of the interaction dynamics and their patterns on the far-field sound generated. Except for the results of intense amplification, the results generally agree with coaxial jets of normal and inverted mean velocity profiles.

Nomenclature

A, α	= constants depending on core vorticity distribution
c_0	= ambient speed of sound
D	= nozzle diameter of circular jet
D_i, D_o	= inner and outer diameters of coaxial jets, respectively
$\boldsymbol{e}_z$	= streamwise unit vector
f	= frequency
$\boldsymbol{n}$	= unit vector normal in the direction of vortex ring propagation
p, $p'_{\max}$, p'_{rms}	= far-field, maximum, and rms pressures, respectively
$p'_{2,\max}$, $p'_{2,\text{rms}}$	= maximum and rms far-field pressures, respectively, two vortex ring system
R	= initial vortex ring radius
r	= radial distance from origin
Sr_D	= Strouhal number, based on jet nozzle diameter D
s	= element arc length on the vortex ring
t	= time in flowfield; retarded time in sound field
$\boldsymbol{U}_I$	= induced velocity on vortex ring
U_i, U_o	= inner and outer jet exit velocities, respectively
$\boldsymbol{U}_T$	= self-induced translational velocity of an isolated vortex ring
$\boldsymbol{V}$	= total propagation velocity of a vortex ring, $\boldsymbol{U}_T + \boldsymbol{U}_I$
V_r, V_z	= radial and streamwise components of vortex ring propagation velocity, respectively
$\boldsymbol{x}$, $\hat{\boldsymbol{x}}$	= far-field displacement and its unit vector, respectively
$\boldsymbol{y}$	= near-field displacement
z	= streamwise distance from origin
æ$_r$, æ$_z$	= radial and streamwise components of vortex ring acceleration, respectively
Γ	= vortex ring circulation
ΔSPL	= sound pressure level difference
λ_{acou}	= acoustic wavelength
λ_c	= initial separation between the pair of control vortex rings
λ_o	= initial phase shift between the control and original trailing vortex rings
λ_T	= initial separation between the pair of original vortex rings
ξ	= angle between far-field displacement and common axis of vortex rings
ρ_0	= density of ambient fluid
σ	= effective vortex ring core radius
τ	= far-field observer time, $t + \lvert\boldsymbol{x}\rvert / c_0$

Subscripts

CL	= leading vortex ring, control vortex ring pair
CT	= trailing vortex ring, control vortex ring pair
i, j	= indices
L	= leading vortex ring, original vortex ring pair
T	= trailing vortex ring, original vortex ring pair

Introduction

IN an initially laminar circular air jet pairings of vortex rings are found as the major activities that form the coherent structures and have been suggested as the sound source.[1–4] Mutual threading, or slip through, of two adjacent vortex rings having circulation of the same sign can be considered as a form of pairing.[5] Based on the vortex filament model, the analytical and numerical results suggest a sound pulse is generated at or near the slip through instant, when the two vortex rings are on the same plane.[2,6] The importance of acceleration and deceleration of the vortex rings, be they of thin- and finite-sized core, in the production of sound was established.[7,8] By defining the vortical structure in a single-jet shear layer as a given pattern in the velocity signal, the experimental results of acceleration showed that acceleration and deceleration of the initial vortical structures were highly related to the production of jet noise.[7] Part of the far-field noise was generated when the trailing vortex ring accelerated and slipped through the leading one. For vortex rings of finite core, besides radial acceleration, axial jerks of their vorticity centroids during their mutual slip through are also important in the sound generation.[8]

Based on a simplified vortex pairing noise model of mutual slip through of two thin planar vortex rings for a low-Mach-number circular jet, the recent numerical results[9] illustrated the eighth power law of Lighthill.[10] The linear relationship of the amplitude of sound with nozzle diameter is also consistent with the existing jet sound theories at 90-deg emission angle. This indicated the importance of the understanding of the pairing of vortical structures on the jet noise generation.

Introduction of a concentric annular jet, forming a coaxial jet, was found to suppress or amplify jet noise.[11–14] In comparison with a fully mixed equivalent single jet,[12] defined as having a uniform exit profile of the same thrust, mass flow rate, and exit area as the coaxial jet, the jets with mean velocity ratio U_o/U_i less than unity

Received 21 April 1998; revision received 5 February 1999; accepted for publication 6 July 1999.

*Professor, Department of Mechanical Engineering.
†Research Fellow, Department of Mechanical Engineering; currently Research Fellow, Department of Mechanical Engineering, Hong Kong Polytechnic University, Hunghom, Kowloon, Hong Kong. Member AIAA.
‡Student, Department of Mechanical Engineering.

are consistently noisier. The coaxial jets with mean velocity ratio greater than unity, the inverted velocity profile, are slightly quieter. The suppression and amplification were found to depend on the mean velocity ratio, area ratio, and frequencies of the components.

The evolution of near-field flow structures in coaxial jets were found, besides the area ratio, to depend on velocity ratio and absolute velocities of the two streams.[15–20] The investigations indicated a variety of widely differing vortex patterns from the two streams. For coaxial jets with mean velocity ratio smaller than unity, the flow dynamics are dominated largely by the vortices that form in the outer shear layer. For those with mean velocity ratio greater than unity, the outer jet also dominates the flow structures. Two flow regimes are identified, depending on whether the mean velocity ratio is smaller or larger than the critical value.[20] For the former, locking between the two layers is found,[19] whereas for the latter, an unsteady recirculation bubble with low-frequency oscillation occurs in the inner jet, approaching that of the limiting case of annular jet.[21–23] Although there was an attempt in correlating the noise characteristics for the special case of an annular jet with its shear layer dynamics[24]; however, there is the absence of detailed study on the noise generation mechanism associated with the flow dynamics of the coherent structures and their complicated interactions.

As the numerical model on the mutual slip through of two thin vortex rings achieves the agreement with the noise generation of single jet,[9] the recent numerical study concerned the effect of the presence of a thin control vortex ring of varying circulation and size on the pairing sound of two identical thin vortex rings.[25] In no background flow case the model mainly concerned their simple interactions, without amalgamation and coalescence, of these thin vortex rings, having the same and opposite sense of rotation. For the control vortex ring of the same sense of rotation, only sound amplification is found. However, amplification and attenuation of sound are possible for the interaction of an opposite sense control vortex ring with the two original pairing rings. Four basic types of vortex ring interactions, out of the large variations of radius ratio, circulation ratio, and separation, resulting in different degrees of amplification and attenuation, were established.

In the initial region, very near the nozzle exit, of coaxial jets, there are two trains of initial vortex rings.[15–17] Thus, the present study extends the investigation to the interaction of two pairs of vortex rings of varying properties and the sound generated. Although the background axisymmetric potential flow and its gradient have been included in another numerical study of vortex ring pairing sound,[26] the simplified axisymmetric vortex model of thin inviscid vortex ring, without the background potential flow, is still adopted. Again, coalescence and amalgamation of the four interacting vortex rings are not considered. As the model used is a simplified one, which is different from the real free shear flows of coaxial jets, making comparison with real flows is difficult. However, the results of the two interacting pairs will be compared with those of a single pair with a control vortex ring and of the available experimental results of coaxial jets.

Model for Coaxial Vortex Ring Pairs and Pairing Sound

The present investigation focuses firstly on the sound generated by the interaction of two vortex ring pairs and then their mutual threading motion. Sound radiation from vortex coalescence or amalgamation, in which any two interacting vortex rings merge, either partially or completely[8] to form a single vortical structure is not considered. During interaction, the axisymmetry of all the vortex rings is preserved. As the pairing of two identical vortex rings and its sound generation, which are used as the basis for quantifying the sound amplification and attenuation caused by the presence of control vortices, have been well documented in previous studies,[9,27] they are not repeated here. An additional pair of identical vortex rings of varying properties is introduced into the original two vortex ring system, and the motion of all vortices, as well as the associated sound generation, is computed (Fig. 1).

The velocity $\boldsymbol{V}_i(V_{z,i}, V_{r,i})$ of the ith vortex ring at position $\boldsymbol{y}_i(z_i, r_i)$ of the four vortex ring system is composed of its self-induced translational velocity $\boldsymbol{U}_{T,i}$, which is its self-propagating velocity because of its finite curvature, and the velocity $\boldsymbol{U}_{I,i}$ caused by mutual induction by other vortices. z_i and r_i, respectively, represent the streamwise and radial coordinates, with the streamwise direction aligning with the self-propagating velocity of the original two vortex ring system. This choice of streamwise direction is consistent with the direction of propagation of vortical structures in the shear layers of axisymmetric jets.[5,15,17] Using the vortex filament model for inviscid and incompressible flow,[2,28] the total velocity $\boldsymbol{V}_i$ of the vortex ring with circulation Γ_i can be expressed as[28]

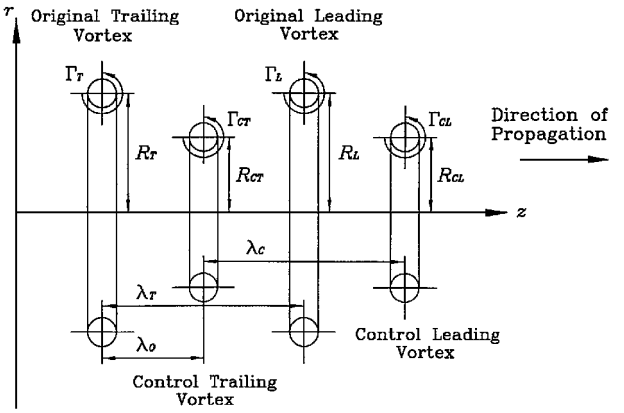

Fig. 1 Schematic diagram of four vortex ring system.

$$\boldsymbol{V}_i = \boldsymbol{U}_{T,i} + \boldsymbol{U}_{I,i} = \frac{\Gamma_i}{4\pi \boldsymbol{R}_i}\left[\log\left(\frac{8\boldsymbol{R}_i}{\sigma_i}\right) - \frac{1}{2} + \boldsymbol{A}\right]\boldsymbol{e}_z$$

$$-\frac{1}{4\pi}\sum_{i\neq j}\int \Gamma_j \frac{\boldsymbol{y}_i - \boldsymbol{y}_j}{(|\boldsymbol{y}_i - \boldsymbol{y}_j|^2 + \alpha\sigma_j^2)} \times \frac{\mathrm{d}\boldsymbol{y}_j}{\mathrm{d}s_j}\,\mathrm{d}s_j \tag{1}$$

where $\alpha = \exp(-1 - 2A)$. For vortex core with uniform vorticity distribution, $A = \frac{1}{4}$ (Refs. 9 and 28). Condition of incompressibility requires the quantity $R_i\sigma_i^2$ be kept constant throughout the entire computation.[9] The position $\boldsymbol{y}_i(z_i, r_i)$ of the ith vortex ring can be obtained by integrating Eq. (1) with respect to time using the fourth-order Runge–Kutta method, and its acceleration $\boldsymbol{æ}_i$ is given by differentiating the position $\boldsymbol{y}_i$ twice with respect to time:

$$\boldsymbol{æ}_i = (æ_{z,i}, æ_{r,i}) = \frac{\mathrm{d}^2}{\mathrm{d}t^2}(z_i, r_i) \tag{2}$$

The far-field sound $p(\boldsymbol{x}, \tau)$ generated by unsteady vortical flow in an unbounded fluid can be obtained by solving the following inhomogeneous wave equation:

$$\nabla^2 p - \frac{1}{c_0^2}\frac{\partial^2 p}{\partial \tau^2} = -\rho_0 \nabla \cdot (\omega \times \boldsymbol{u}) \tag{3}$$

For an acoustically compact low-Mach-number flow, where all of the characteristic flow velocities and lengths of the vortical region are small in comparison with the ambient speed and wavelength of the generated sound, the whole fluid domain can be separated into a near vortical flow field and a far acoustic field. Möhring[2] formulates an integral convolution solution to Eq. (3) with a vector Greens function and obtains

$$p(x, \tau) = \frac{\rho_0}{12\pi c_0^2 |\boldsymbol{x}|^3}\frac{\partial}{\partial t}\int (\boldsymbol{x}\cdot\boldsymbol{y})\boldsymbol{y}\cdot(\omega\times\boldsymbol{x})\,\mathrm{d}^3\boldsymbol{y} \tag{4}$$

where the integrand and time differentiation are evaluated at the retarded time t, where $t = \tau - |\boldsymbol{x}|/c_0$. For a system of thin vortex rings moving along a common axis parallel to unit vector $\boldsymbol{n}$, the sound pressure fluctuations $p(\boldsymbol{x}, \tau)$ at a distance $\boldsymbol{x}$ in the far field are of the form[2]

$$p(\boldsymbol{x}, \tau) = \frac{\rho_0}{4c_0^2|\boldsymbol{x}|^3}\left[\boldsymbol{x}\cdot\left(\boldsymbol{nn} - \frac{1}{3}\right)\cdot\boldsymbol{x}\right]\frac{\mathrm{d}^3 Q}{\mathrm{d}t^3}$$

$$= \frac{\rho_0}{4c_0^2|\boldsymbol{x}|}\left(\cos^2\xi - \frac{1}{3}\right)\frac{\mathrm{d}^3 Q}{\mathrm{d}t^3} \tag{5}$$

where $Q = \Sigma_i \Gamma_i R_i^2 z_i$ and ξ is the angle between the far-field observer direction $\boldsymbol{n}$ and the common axis with $\cos\xi = \hat{\boldsymbol{x}}\cdot\boldsymbol{n}$. Equation (5)

shows that the amplitude of the far-field sound pressure fluctuations is dependent on the third time derivative of vortex properties Q only. The sound field has the directivity of that produced by a quadrupole in the $\boldsymbol{n}$ direction, together with an isotropic quadrupole, as revealed in the bracketed terms in Eq. (5) (Ref. 2). In the following sections only the sound pressure fluctuations at zero ξ will be presented.

The parameters that affect the vortex ring interactions, thus, the sound generation, are the initial vortex ring circulations Γ_T and Γ_c, initial vortex ring radii R_T and R_c, and initial separations of the vortices λ_T and λ_c of the vortex ring pairs. The regime of study covers $0.5 \leq R_c/R_T \leq 2.0$, $-1.75 \leq \Gamma_c/\Gamma_T \leq -0.01$, and $0.01 \leq \Gamma_c/\Gamma_T \leq 2.00$, $0.25 \leq \lambda_c/\lambda_T \leq 2.0$. The initial separation of the original vortex pair λ_T is set equal to R_T. The relative positions or phase shift between the two pairs of vortices is λ_o/λ_T. The range of λ_o/λ_T covers 0, 0.25, 0.5, 0.75, and 1. The core-to-ring-radius ratios of all vortex rings are 0.1. All together, there were 5760 cases computed. Throughout the study the properties of the initially trailing vortex ring, namely Γ_T and R_T, are selected as the normalization references. The normalized time, velocity, and acceleration are $t' = t/(R_T^2/\Gamma_T)$, $\boldsymbol{V}' = \boldsymbol{V}/(\Gamma_T/R_T)$, and $\boldsymbol{æ}' = \boldsymbol{æ}/(\Gamma_T^2/R_T^3)$, respectively. The normalized frequency f' is $1/t'$. For unity density the normalized sound pressure is $p' = p/(\Gamma_T^2/R_T^2)$. The computation was carried out at $0 \leq t' \leq 50$. The spatial integration along the periphery of the vortex ring is done by Simpson's method with 360 segments.[25] The normalized time step used in the computation is $\Delta t' = 0.02$. Several smaller values of $\Delta t'$ and more spatial segments for each vortex ring have been attempted, but no observable change of the results was found.

Results and Discussion

As have been presented,[25] the maximum normalized far-field pressure $p'_{2,\max}$ of the original two vortex ring system within the time span of $0 \leq t' \leq 50$ is 0.715, and its rms sound pressure $p'_{2,\mathrm{rms}}$ is 0.21. The maximum sound pressure is radiated at the instant of the occurrence of the slip through process at which high acceleration or deceleration of the two vortices are found.

With the introduction of the control vortex ring pair, the amplification and attenuation of the far-field sound pressure level, based on the rms pressure p'_{rms}, $\Delta\mathrm{SPL} = 10\log_{10}(p'^2_{\mathrm{rms}}/p'^2_{2,\mathrm{rms}})$ in dB, in comparison with that of original two vortex rings within the regime of study have been computed. The adoption of the rms sound pressure p'_{rms} is because of its relation to the sound power explicitly, if the sound source is steady or within a short time interval. As there are a lot of results, only three representative isocontours of the chosen parameters are shown in Figs. 2a–2c, indicating the maximum attenuation, the maximum amplification and that between these two extremes, respectively. For $\lambda_c/\lambda_T = 1$, as the core-to-ring radius ratio of the vortex ring is 0.1, the results at which two vortex rings initially overlap are not properly handled by the present model and, thus, not presented (Fig. 2a). For the isocontours the solid lines indicate attenuation of sound pressure caused by the presence of the control vortex pair, and the dotted lines indicate amplification. Generally, Figs. 2a–2c show that attenuation ΔSPL is mainly found at ring radius ratio $R_c/R_T > 1$ and in the first quadrant for the control vortex pair with the oppositely sensed circulation ($-1 < \Gamma_c/\Gamma_T < 0$). It is at $\lambda_c/\lambda_T = 1.25$, $\lambda_o/\lambda_T = 0.5$ that a region of minor attenuation in the second quadrant for the control vortex ring pair with the same sensed circulation (Fig. 2c). Amplification is found at other quadrants, particularly for interaction with the same sensed control vortices.

The maximum attenuation of the far-field sound pressure level is about -13 dB at $\lambda_c/\lambda_T = 1.0$, $\lambda_o/\lambda_T = 0$, $\Gamma_c/\Gamma_T = -0.50$, $R_c/R_T = 1.75$, and is marked as moderate attenuation (MR) (Fig. 2a). Its magnitude is significantly lower than the maximum amplification of about +85 dB at $\lambda_c/\lambda_T = 0.25$, $\lambda_o/\lambda_T = 0.5$, $\Gamma_c/\Gamma_T = 2.0$, $R_c/R_T = 1.25$, and is marked as intense amplification (IA) (Fig. 2b). The maximum attenuation is found with the oppositely sensed control vortex pair of half circulation ($\Gamma_c/\Gamma_T = -0.5$), the same vortex separation ($\lambda_c/\lambda_T = 1.0$), no phase shift ($\lambda_o/\lambda_T = 0$), and ring radius ($R_c/R_T = 1.75$) significantly larger than the original vortex pair. The maximum amplification is found with the same sensed control vortex pair of higher circulation ($\Gamma_c/\Gamma_T = 2.0$), much smaller vortex separation ($\lambda_c/\lambda_T = 0.25$), larger phase shift with the trailing control vortex ($\lambda_o/\lambda_T = 0.5$), and bigger ring radius ($R_c/R_T = 1.25$) than the original vortex pair. Generally, the high sound pressure amplification of over +80 dB is found at this small vortex separation ($\lambda_c/\lambda_T = 0.25$) of the control vortices of the same direction of rotation and of high circulation ($\Gamma_c/\Gamma_T \geq 1.75$). One of the control vortices is adjacent to either vortex of the original pair.

A representative moderate amplification (MA) of +9 dB at $\lambda_c/\lambda_T = 1.25$, $\lambda_o/\lambda_T = 0.5$, $\Gamma_c/\Gamma_T = -0.75$, $R_c/R_T = 1.0$, and

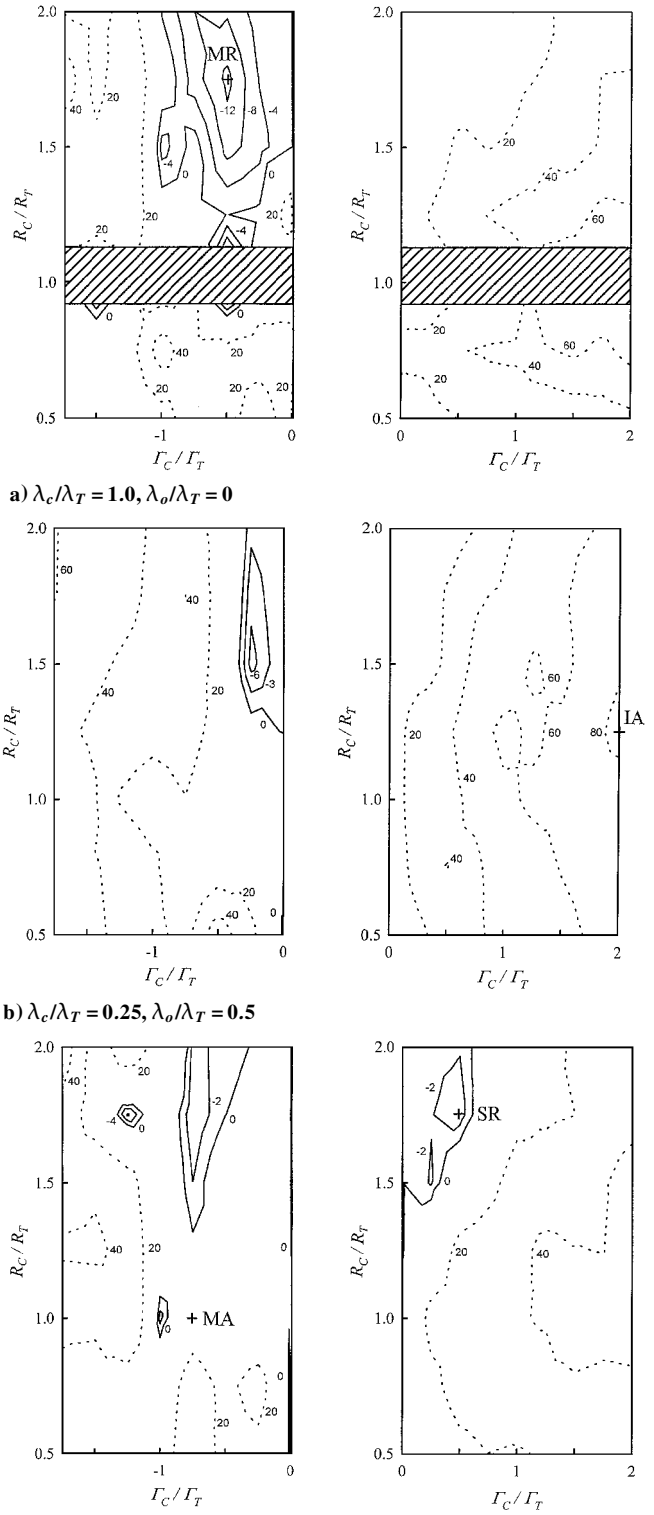

a) $\lambda_c/\lambda_T = 1.0$, $\lambda_o/\lambda_T = 0$

b) $\lambda_c/\lambda_T = 0.25$, $\lambda_o/\lambda_T = 0.5$

c) $\lambda_c/\lambda_T = 1.25$, $\lambda_o/\lambda_T = 0.5$

Fig. 2 Isocontours of difference of far-field sound pressure: ——, attenuation, and · · · ; amplification. Figure represents ± dB. Regions where vortex cores overlap are hatched.

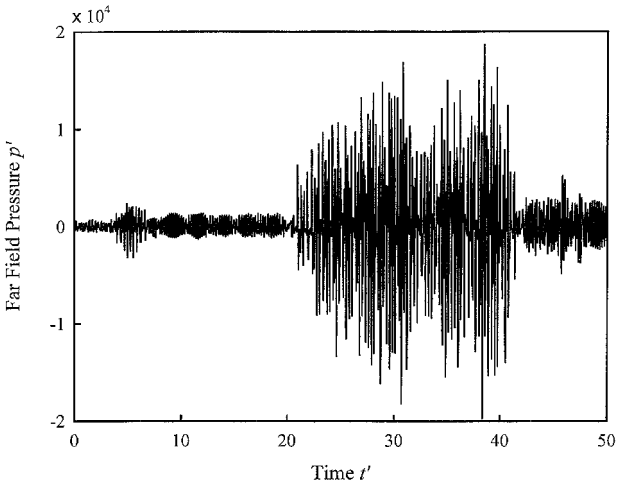

Fig. 3 Far-field sound pressure at intense amplification. Control vortex pair: $\lambda_c/\lambda_T = 0.25$, $\lambda_o/\lambda_T = 0.5$, $\Gamma_c/\Gamma_T = 2.0$, and $R_c/R_T = 1.25$.

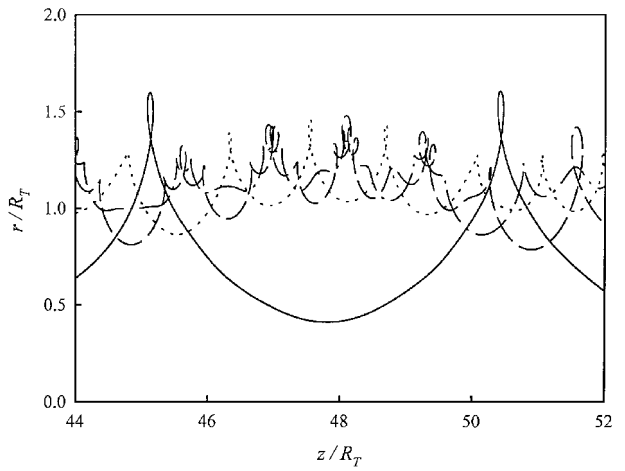

Fig. 4 Locations of four interacting vortex rings at intense amplification: – – –, leading vortex ring; ——, trailing vortex ring; · · ·, control leading vortex ring; and – ∽ –, control trailing vortex ring. Control vortex pair: $\lambda_c/\lambda_T = 0.25$, $\lambda_o/\lambda_T = 0.5$, $\Gamma_c/\Gamma_T = 2.0$, and $R_c/R_T = 1.25$.

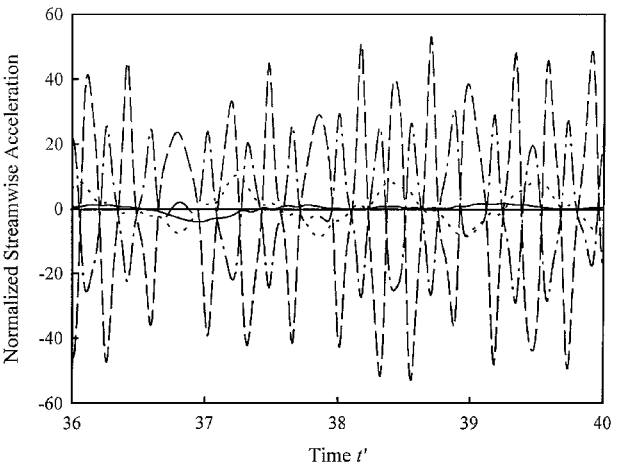

a) Streamwise acceleration

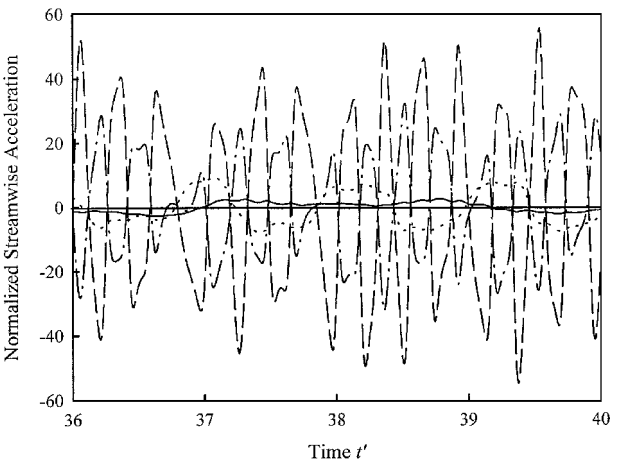

b) Radial acceleration

Fig. 5 Time variations of accelerations of vortex rings at intense amplification: – – –, leading vortex ring; ——, trailing vortex ring; · · ·, control leading vortex ring; and – ∽ –, control trailing vortex ring. Control vortex pair: $\lambda_c/\lambda_T = 0.25$, $\lambda_o/\lambda_T = 0.5$, $\Gamma_c/\Gamma_T = 2.0$, and $R_c/R_T = 1.25$.

small attenuation (SR) of −3 dB at $\lambda_c/\lambda_T = 1.25$, $\lambda_o/\lambda_T = 0.5$, $\Gamma_c/\Gamma_T = 0.5$, $R_c/R_T = 1.75$, are shown in Fig. 2c. The control vortex, be it the leading or trailing one, is farther away from the original vortex pair and of lower circulation.

For the IA the nondimensional far-field sound pressure p' with nondimensionaltime t' at $\lambda_c/\lambda_T = 0.25$, $\lambda_o/\lambda_T = 0.5$, $\Gamma_c/\Gamma_T = 2.0$, $R_c/R_T = 1.25$ is shown in Fig. 3. Within the time span of the present study $0 \le t' \le 50$, there are peaks of extremely high pressure at $20 < t' < 41$. The magnitude of peak sound pressures is as high as about 2×10^4 and are of higher frequencies. The preceding phenomena suggest the presence of the control vortex pair results in very intense far-field sound pressure generation of high frequencies.

The paths of the four vortex rings at IA within $36 \le t' \le 40$ are shown in Fig. 4, in which very vigorous vortex interactions occur. In this case the control vortex rings of the same sense of rotation are so situated that they are very close to the original leading vortex ring, leading to very strong mutual induction and vigorous interactions. The original leading vortex and control trailing vortex appear to spin about each other so rapidly that they convect as a single vortical structure. This vortical structure in turn interacts with the control leading vortex. The successive rapid vortex interactions lead to the generation of high-frequency fluctuations of sound pressure (Fig. 3). The control leading ring involves in lower-frequency interactions, and the interactions of the original trailing ring are of even lower frequency. These different interactions result in different accelerations of the four vortex rings (Figs. 5a and 5b). The magnitude of normalized acceleration of the original leading ring, both the streamwise and radial, is the highest of about 50, whereas that of the control trailing ring is about 30. They correspond to the high-frequency interactions shown in Fig. 4. The magnitude of acceleration of the control leading vortex ring is lower by about 10 and of the original trailing ring by about 4. Even the lowest of the four is still much higher than that of the original vortex pair of about 0.3 (Ref. 25). The phenomena imply that the intense far-field sound pressure is caused mainly by the high-frequency interaction of the original leading and control trailing vortex rings and their associated high accelerations.

For the MA of +9 dB at $\lambda_c/\lambda_T = 1.25$, $\lambda_o/\lambda_T = 0.5$, $\Gamma_c/\Gamma_T = -0.75$, $R_c/R_T = 1.0$, the presence of the control vortex pair results in high peak pressures caused by the interactions of the original trailing and control trailing vortex rings and then of the original leading and control leading vortex rings at $t' < 5$ (Figs. 6a and 7). At $t' > 5$ the peaks are caused by the slip throughs of the control leading and control trailing vortex rings of lower circulation and their convection upstream. Its frequency is lower.

For slight attenuationat SR of −3 dB ($\lambda_c/\lambda_T = 1.25$, $\lambda_o/\lambda_T = 0.5$, $\Gamma_c/\Gamma_T = 0.5$, $R_c/R_T = 1.75$), the peak pressures are +0.49 and −0.19 at $t' < 5$ (Fig. 6b) because of the interactions of the original trailing and control trailing vortex rings and then of the original leading and control leading vortex rings (Fig. 8). After the initial interactions at $t' < 5$, the repetitive slip throughs of lower frequency of the original leading and trailing vortex rings are found.

For moderate attenuation at MR of −13 dB ($\lambda_c/\lambda_T = 1.0$, $\lambda_o/\lambda_T = 0$, $\Gamma_c/\Gamma_T = -0.50$, $R_c/R_T = 1.75$), the peak pressures of +0.36 at $t' = 7$ is caused by the first slip through of the two control

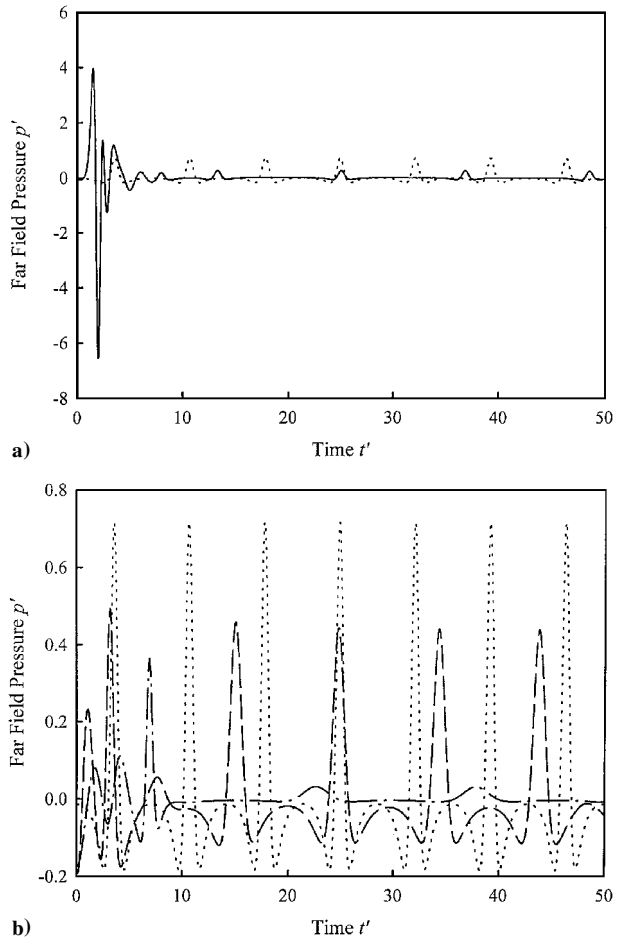

Fig. 6 Far-field sound pressure: a) ——, moderate amplification; control vortex pair: $\lambda_c/\lambda_T = 1.25$, $\lambda_o/\lambda_T = 0.5$, $\Gamma_c/\Gamma_T = -0.75$, and $R_c/R_T = 1.0$; b) – – –, slight attenuation; control vortex pair: $\lambda_c/\lambda_T = 1.25$, $\lambda_o/\lambda_T = 0.5$, $\Gamma_c/\Gamma_T = 0.5$, and $R_c/R_T = 1.75$; – ⌣ –, moderate attenuation; control vortex pair: $\lambda_c/\lambda_T = 1.0$, $\lambda_o/\lambda_T = 0$, $\Gamma_c/\Gamma_T = -0.50$, and $R_c/R_T = 1.75$. · · ·, two-vortex-ring system.

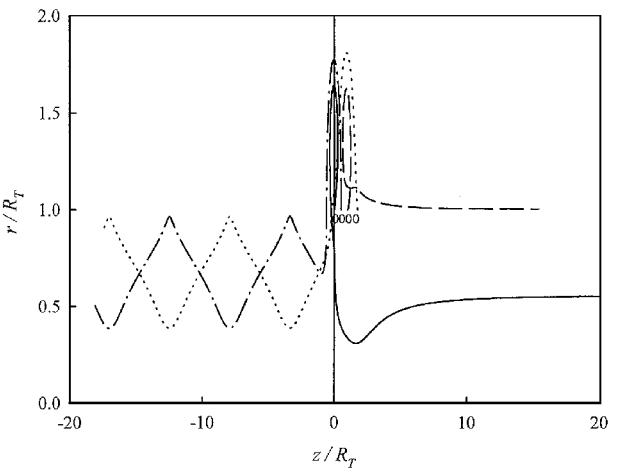

Fig. 7 Locations of four interacting vortex rings at moderate amplification: – – –, leading vortex ring; ——, trailing vortex ring; · · ·, control leading vortex ring; and – ⌣ –, control trailing vortex ring. Control vortex pair: $\lambda_c/\lambda_T = 1.25$, $\lambda_o/\lambda_T = 0.5$, $\Gamma_c/\Gamma_T = -0.75$, and $R_c/R_T = 1.0$.

vortex rings (Figs. 6b and 9). At $t' > 7$ the low sound pressure peaks are caused by the repetitive slip throughs of the two control rings of low circulation. The absence of the slip through of the original vortex pair and the nearly zero pressure of those of the control vortex pair are the cause for the significant attenuation.

The power spectra of the far-field sound pressure of the preceding four representative cases and of the two-vortex-ring system are illustrated in Fig. 10. The broad spectrum of MR does not have the

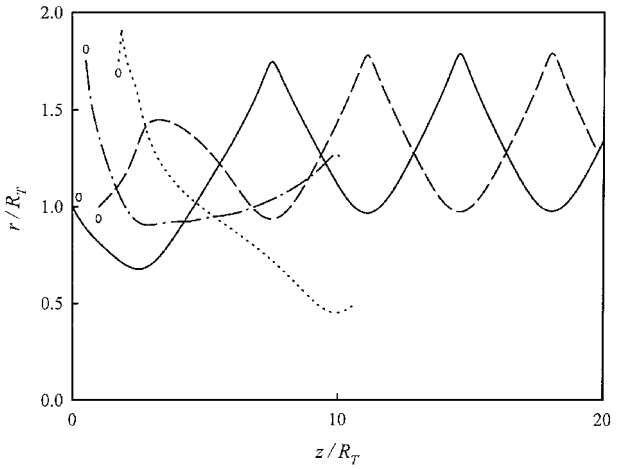

Fig. 8 Locations of four interacting vortex rings at slight attenuation: – – –, leading vortex ring; ——, trailing vortex ring; · · ·, control leading vortex ring; and – ⌣ –, control trailing vortex ring. Control vortex pair: $\lambda_c/\lambda_T = 1.25$, $\lambda_o/\lambda_T = 0.5$, $\Gamma_c/\Gamma_T = 0.5$, and $R_c/R_T = 1.75$.

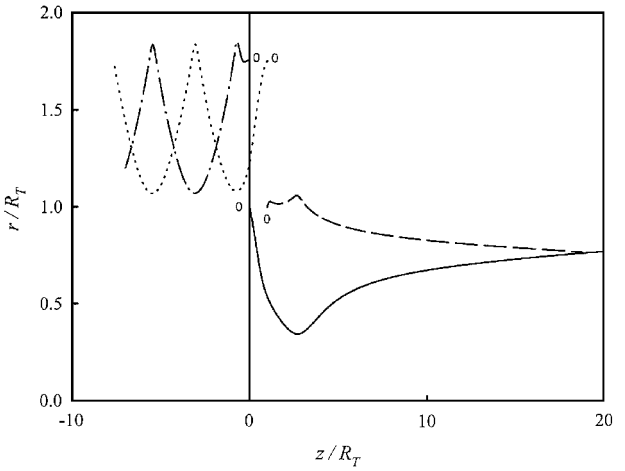

Fig. 9 Locations of four interacting vortex rings at moderate attenuation: – – –, leading vortex ring; ——, trailing vortex ring; · · ·, control leading vortex ring; and – ⌣ –, control trailing vortex ring. Control vortex pair: $\lambda_c/\lambda_T = 1.0$, $\lambda_o/\lambda_T = 0$, $\Gamma_c/\Gamma_T = -0.50$, and $R_c/R_T = 1.75$.

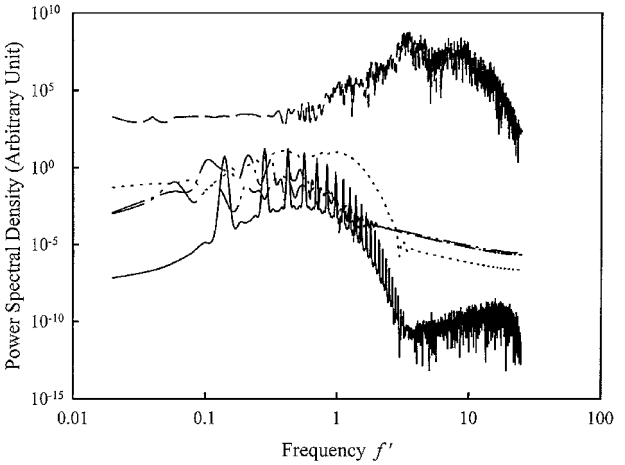

Fig. 10 Spectra of far-field sound pressure: ——, two-vortex-ring system; – – –, IA; · · ·, MA; – ⌣ –, SR; and – · ⌣ · –, MR.

Table 1 Comparison of sound generation of two-vortex, three-vortex, and four-vortex systems

	MR		SR		IA		MA	
System	p'_{max}	ΔSPL, dB	p'_{max}	ΔSPL, dB	p'_{max}	ΔSPL, dB	p'_{max}	ΔSPL, dB
Two vortex[25]	+0.715	0	——	——	——	——	——	——
	−0.184	——	——	——	——	——	——	——
Three vortex[25]	+0.30	−15	+0.36	−10	$+3\times10^3$	+55	+2.4	+10
	−0.10	——	−0.17	——	-7.55×10^3	——	−0.6	——
Four vortex	+0.36	−13	+0.49	−3	$\pm2\times10^4$	+85	+4.0	+9
	−0.17	——	−0.19	——	——	——	−6.5	——

discrete spectral peaks and of lower level than that of SR. The latter has more discrete peaks, but its spectral level is lower than that of the two-vortex-ring system. The spectrum of MA has higher levels and more higher-frequency components than those of two-vortex system. The spectrum of IA tends to be broad and has significant increase in the high-frequency components.

An important assumption of the low-Mach-number aerodynamic sound theory is the ratio of the characteristic dimension of the sound generating flow, the R_T in the present study, to the acoustic wavelength λ_{acou} being much smaller than unity, i.e., $R_T/\lambda_{acou} \ll 1$ (Refs. 2, 6, and 10). For $R_T \approx \lambda_{acou}$ the normalized frequency of radiation f' might possibly have the relationship of $f' \approx c_0 R_T/\Gamma$. Leung et al.[9] proposed a relation between the vortex circulation and the jet flow velocity U as $\Gamma = kUDSr_D^{-1/3}$, where k is a constant and $D \approx 2R_T$ the nozzle diameter. After some simple mathematics the frequency is

$$f' \approx c_0/kU \tag{6}$$

Typical experimental values of k and U are 1.11 and 50 m/s, respectively.[9] Substituting these values into Eq. (6), one gets an estimate for $f' \approx 30$. All power spectra shown in Fig. 10 fall below this limit. Thus, the sound computation for all cases in the present study is acoustically compact under the context of low-Mach-number aerodynamic noise theory, although the dominating high-frequency peaks emerge in the cases similar to the IA.

The p'_{max} and ΔSPL of the original two-vortex system, the three-vortex system,[25] and the present four-vortex system are tabulated in Table 1. For the MR the present four-vortex system has slightly higher p'_{max}, thus smaller attenuation by about 2 dB. However, both systems have peak pressures lower than those of the original two-vortex system because of the suppression of the slip through of the original vortex pair by the control vortex pair of lower circulation. For the SR the smaller attenuation than that of the MR is associated with the weaker suppression of the slip throughs of the original vortex pair by the control vortex pair. However, the control pair still plays its role in suppressing the interaction of the original vortex rings, though to a lesser degree.

With the introduction of the control vortex pair, amplification of the far-field pressure is found, as long as the control vortex rings have comparable or greater circulation than those of the original vortex pair. The present four-vortex system has significantly higher amplification for the IA than the three-vortex system, by as much as +30 dB, because of the rapid interaction and the associated accelerations of the adjacent original and control vortex rings.

For the MA, though the circulation of the control vortex pair is comparable to that of the original vortex pair, its initial vortex separation and its location with the original vortex pair, then, play their role in the interaction. The slip throughs of the adjacent vortex rings, be they of the original or control rings of comparable circulation, are similar or more intense than the two vortex system.

Experiments devoted to explore the relationship between the dynamics of the flow structures in the near field of coaxial jets and the associated sound generation are scare. Thus, direct comparison with the present findings is not possible. However, although the present investigation is based on no mean flow, the present results still provide some insight into the mechanism of noise generation of coaxial jets, in which the initial vortex rings play a significant role. As the single-jet sound generation could be predicted by the simple model of pairing of two vortex rings,[9] the introduction of a control vortex ring proved to be reasonably successful in predicting the trend of the noise attenuation of inverted velocity profile coaxial jets.[25]

Flow visualization of coaxial jets of mean velocity ratios $1 < U_o/U_i < 6.67$ and nozzle exit diameter ratio 2 at the Reynolds numbers, based on the outer jet diameter, $1\times10^4 \le Re_{Do} \le 4\times10^4$ indicated the presence of outer vortices and their coalescence in the outer mixing region.[16] For $U_o/U_i \le 1.25$ the alternating vortices shed behind the inner nozzle lip are the only one present. For $U_o/U_i > 2$ the inner vortices, which have an opposite sense of rotation to that of the outer vortices, are dominant. Coalescence of these inner vortices and their evolution into another train of vortices that resembles the wake vortices found in the annular jet are observed.[16,18] For $1.25 < (U_o/U_i)^{-1} < 2$ both the alternating wake and shear layer structures are present. Farther downstream from the nozzle exit, there is interaction of the outer and inner vortices of the two types.

The flow visualization, nearly of the same Reynolds number, was based on the coaxial jets of nozzle exit diameter ratio 1.4 (Ref. 17). As the initial instability and subsequent roll up at each interface are closer than those of Au and Ko[16] because of the difference in the mutual induction of the vortices, one would expect earlier and more extensive interactions of the vortices from the two more adjacent shear layers.[17] For the coaxial jets of $U_o/U_i \le 1$, the outer vortices are always present.[17] However, at $U_o/U_i = 1.14$ a locking between the two shear layers is evident, and the inner layer does not seem to roll up into vortices. For $2.56 \le U_o/U_i \le 4.16$ the inner layer rolls up to form shear-layer vortices with opposite sense of circulation. The locking of the two layers produces a cyclic interaction between the two types of vortices.

The visualization study of coaxial jets of nozzle exit diameter ratio 1.35 also showed that the outer vortices, which dominate the flow dynamics, are insensitive to the mean velocity ratio $2 \le U_o/U_i \le 4$ (Ref. 20). The two mixing layers, as found by the preceding workers,[16–18] develop independently of each other, and the two types of flow structures interact near the end of the outer potential core. Even at $U_o/U_i > 8$, higher than the critical value at which the near-field flow pattern is characterized by the formation of a recirculating flow cavity of wake-type structure, the roll-up outer and inner structures are still found to interact.[20] Even with the limiting case of annular jet, the inner vortices are still observed.[22–24]

For $U_o/U_i < 1$ the outer vortices are also dominant.[15,17] For the inner mixing layer an inner train of vortices was shown.[15] However, the recent results at $U_o/U_i = 0.59$ and 0.71 only indicated the indication of instability of the inner layer, and it has not rolled up into vortical structures.[17] This instability seems to be affected by the outer vortices. The difference in the observations of the inner mixing layer and the subsequent roll up into vortices may be caused by the difference in the inner boundary layer at the inner nozzle exit and in the nozzle exit diameter ratio at which the mutual induction of vortical structures may play its part.

Thus, instead of the addition of a single control vortex ring, the present system of two vortex ring pairs gives a better simulation of the coaxial jet near-field flow dynamics. Although the two potential flow streams and their mean shears are not included, the flow visualization of coaxial jets of lower Reynolds number $Re_D = 1.67\times10^3$ showed interaction of the two adjacent, still distinct, vortex ring pairs from the outer and inner mixing layers at $z/D_o \approx 1$ (Ref. 29). At $\lambda = 1.67$ the four vortex rings of distinct identities undergo interaction at $z/D_o \approx 1$ and farther downstream. The numerical study

on the effect of the presence of a background axisymmetric potential flow on the pairing of two coaxial vortex rings showed that the flow affects substantially the sound generation process in the beginning of their interaction.[26] The mean shear rate increases the sound generated when the vortex rings are interacting within the region of high mean shear. However, because of nonzero divergence, the mean velocity profile of a practical jet could not be used. Rather, a potential flow based on the Bessel functions of the first kind of the zero and first order was adopted.[30] This illustrates the difficulty in modeling with a real jet mean velocity profile, not mentioning two profiles of different velocities and mean shear.

Nevertheless, the present simplified model predicts amplification and attenuation of the sound generated for the control vortex ring pair having the positive and negative circulation. For coaxial jets of normal velocity profile ($U_o/U_i < 1$), the experimental results indicated a reduction in the overall sound pressure level, relative to the noise from the inner jet at $0 < U_o/U_i < 0.75$ (Refs. 11 and 31). A maximum noise reduction is about -3 to -5 dB at $U_o/U_i \approx 0.5$. At $0.75 < U_o/U_i < 1$ increase in noise is found. By adopting the fully mixed equivalent jet, having a uniform exit profile and the same exit area, mass flow rate and thrust as the coaxial jets,[12] the coaxial jets with normal velocity profile are noisier. However, in the present study, the sound generated by the interaction of the four vortex ring system is compared with that of the original vortex pair. It seems to be more appropriate to compare the present results with those of coaxial jets having a single jet as the reference.[11,31] The present SR of -3 dB is found at $\Gamma_c/\Gamma_T = 0.5$ and $R_c/R_T = 1.75$ (Fig. 2c), at which the same sense of rotation and the radii of the control and original vortex rings correspond to the vortices within the coaxial jets of normal mean velocity profile. The present attenuation of -3 dB is also comparable with the maximum reduction of -3 to -5 dB of coaxial jets at $U_o/U_i \approx 0.5$ (Refs. 11 and 31).

For the same sensed control and original vortices the IA at $\Gamma_c/\Gamma_T = 2.0$ of $+85$ dB is much higher than about $+6$ dB of coaxial jets of normal mean velocity profile of $U_o/U_i \approx 0.95$ (Refs. 11 and 31), mainly because of the intense and rapid interactions of the same sensed vortices shortly after the start of computation (Fig. 3). Later, these interactions can further be intensified and produce higher pressure fluctuations. The assumption of no coalescence and amalgamation of these interacting vortices, allowing their continuous intense interactions, is the main cause for such large discrepancy.

Moderate amplification, at $5 < \Delta\text{SPL} < 20$ dB, is also found at $\Gamma_c/\Gamma_T > 1$ of the same sense of direction of rotation of both the control and original vortices. The regime is generally smaller than that at $\Gamma_c/\Gamma_T < 0$ of opposite sense of rotation (Figs. 2a–2c). At the MA with $\Gamma_c/\Gamma_T = -0.75$, the increase is $+9$ dB for $0 < t' \leq 50$. This increase, as other cases in this regime of moderate amplification, is mainly caused by the high transient increase in the beginning of the interactions (Figs. 6a and 7). For $2 \leq t' \leq 50$ the increase is only $+4.7$ dB, and for $3 \leq t' \leq 50$ attenuation of -2.9 dB is found.

For coaxial jets of mean velocity ratio less than unity, at $U_o/U_i = 0.95$ the amplification is about $+5$ dB (Refs. 11 and 31). At velocity ratio greater than unity, the amplification is about $+5$ to $+9$ dB at $U_o/U_i \approx 1.2$ (Refs. 11 and 12). This is comparable with the MA of $+9$ dB of the present study. This general agreement may be caused by the present model of thin vortex rings that can simulate the interactions of the initial vortex rings, soon after their roll up and are still of small core sizes before their pairings.

The regime of moderate attenuation, with the MR of -13 dB, is mainly found in the quadrant of negative circulation ratios $0 > \Gamma_c/\Gamma_T > -1$ and radius ratio $1 < R_c/R_T < 2$ (Figs. 2a–2c). In this quadrant the control and original vortex rings have the opposite sense of rotation. This corresponds to the coaxial jets of inverted mean velocity profiles of $U_o/U_i > 1$. By comparing the coaxial jet noise level with that of $U_o/U_i = 1$, a reduction of 10 dB in normalized overall sound power level is obtained when the U_o/U_i is increased from 1 to 2 (Ref. 12). When compared with either the fully mixed equivalent jet or the jet of total thrust being maintained constant, the maximum reduction is 3 to 4 dB at $U_o/U_i \approx 1.5$ (Ref. 12). Thus, the present moderate attenuation is comparable with those of coaxial jets.

The coaxial jets with inverted velocity profiles are quieter, whereas those with normal profiles noisier. This phenomenon is also indicated by the present results that the amplification and attenuation in the regime of negative circulation ratio are generally lower than those in the regime of positive circulation ratio. Further, for the coaxial jets of inverted mean velocity profiles, the one-third octave sound pressure level spectra show a reduction in the pressure level at low frequencies and an increase at higher frequencies with the increase from $U_o/U_i = 1.00$ to 1.75 (Ref. 12). The spectra shown in Fig. 10 indicate for the MR and SR the increase in levels at high frequencies from the two-vortex system is caused by the intense and rapid interactions of adjacent vortex rings. At low frequencies there is also a reduction in level, especially for the MR. These phenomena agree with the trend of coaxial jets.

For coaxial jets of normal mean velocity profile, the noise reduction also depends on area ratio.[11,12] As discussed on the flow visualization results, the differences in the state of development of the instability within the inner shear layer, its roll up, and the effect of mutual induction caused by the outer vortex rings may be the cause for the difference in noise reduction. As indicated by the present study, the relative positions of the individual control and original vortex rings, caused by the radius ratio R_c/R_T, separation ratio λ_c/λ_T, and phase λ_o/λ_T, affect the sound generated and their amplification or attenuation (Figs. 2a–2c). However, the present model deals only with vortex rings, whereas the coaxial jets may still have their shear layers and the instability has not yet rolled up to form the initial vortex rings.[17]

Conclusion

Based on a numerical study of the interactions of two pairs of two coaxial thin vortex rings of the same and opposite circulation, different varieties of widely different near-field vortex interaction patterns are found. These interaction patterns depend on the circulation ratio, radius ratio, separation ratio, and phase of these two interacting pairs.

Out of these different varieties of patterns and their associated far-field sound generation, four basic types of interaction with different degrees of amplification or attenuation are established. The intense amplification is caused by the very rigorous and rapid interaction and significant increase in the acceleration of the interacting vortices. The moderate amplification is the result of initial enhanced interaction. For attenuation the slight attenuation is caused by the slight suppression of the original two vortex rings by the control vortex pair and their subsequent repetitive slip throughs. For moderate attenuation the control vortices suppress the initial interaction and the subsequent slip throughs, resulting in lower far-field sound.

In comparison with three-vortex system, the present system of two control vortex rings generally results in significantly higher amplification and slightly smaller attenuation, which is mainly caused by the second control vortex ring that offers another opportunity for interaction. This illustrates the contribution of interaction of vortices to the generation of sound and the importance of the understanding of the structures of vortex patterns and the dynamics of their interaction. The present simple model of four thin interacting rings shows general agreement with the noise generation of coaxial jets of both normal and inverted mean velocity profiles, in which the very rapid and intense interactions are not continuous.

References

[1] Winant, C. D., and Browand, F. K., "Vortex Pairing: The Mechanism of Turbulent Mixing-Layer Growth at Moderate Reynolds Numbers," *Journal of Fluid Mechanics*, Vol. 63, Pt. 2, 1974, pp. 237–255.

[2] Möhring, W., "On Vortex Sound at Low Mach Number," *Journal of Fluid Mechanics*, Vol. 65, No. 4, 1978, pp. 685–691.

[3] Kibens, V., "Discrete Noise Spectrum Generated by an Acoustically Excited Jet," *AIAA Journal*, Vol. 18, No. 4, 1980, pp. 434–441.

[4] Laufer, J., and Yen, T., "Noise Generation by a Low Mach Number Jet," *Journal of Fluid Mechanics*, Vol. 134, 1983, pp. 1–31.

[5] Yamada, H., and Matsui, T., "Mutual Slip-through of a Pair of Vortex Rings," *Physics of Fluids*, Vol. 22, No. 7, 1979, pp. 1245–1249.

[6] Kambe, T., and Minota, T., "Sound Radiation from Vortex Systems," *Journal of Sound and Vibration*, Vol. 74, No. 1, 1981, pp. 61–72.

[7]Tang, S. K., and Ko, N. W. M., "A Study on the Noise Generation Mechanism in a Circular Jet," *Journal of Fluids Engineering*, Vol. 115, No. 3, 1993, pp. 425–435.

[8]Tang, S. K., and Ko, N. W. M., "On Sound Generated from the Interaction of Two Inviscid Coaxial Vortex Rings Moving in the Same Direction," *Journal of Sound and Vibration*, Vol. 187, No. 2, 1995, pp. 287–310.

[9]Leung, R. C. K., Tang, S. K., Ho, I. C. K., and Ko, N. W. M., "Vortex Pairing as a Model for Jet Noise Generation," *AIAA Journal*, Vol. 34, No. 4, 1996, pp. 669–677.

[10]Lighthill, M. J., "On Sound Generated Aerodynamically: II. Turbulence as a Source of Sound," *Proceedings of the Royal Society of London, Series A*, Vol. 222, 1954, pp. 1–32.

[11]Williams, T. J., Ali, M. R. M. H., and Anderson, J. S., "Noise and Flow Characteristics of Coaxial Jets," *Journal of Mechanical Engineering Science*, Vol. 11, No. 2, 1969, pp. 133–142.

[12]Tanna, H. K., "Coannular Jets—Are They Really Quiet and Why?" *Journal of Sound and Vibration*, Vol. 72, No. 1, 1980, pp. 97–118.

[13]Kuznetsov, V. M., and Munin, A. G., "Coaxial Jet Noise and Isothermal Jets," *Soviet Physics Acoustics*, Vol. 24, No. 6, 1978, pp. 498–502.

[14]Gliebe, P. R., Brausch, J. F., Majjigi, R. K., and Lee, R., "Jet Noise Suppression," *Aeroacoustics of Flight Vehicles. Theory and Practice, Vol. 2: Noise Control*, edited by H. H. Hubbard, Acoustical Society of America, New York, 1995, Chap. 15, pp. 207–270.

[15]Kwan, A. S. H., and Ko, N. W. M., "Coherent Structures in Subsonic Coaxial Jets," *Journal of Sound and Vibration*, Vol. 48, No. 2, 1976, pp. 203–219.

[16]Au, H., and Ko, N. W. M., "Coaxial Jets of Different Mean Velocity Ratios," *Journal of Sound and Vibration*, Vol. 100, No. 2, 1985, pp. 211–232.

[17]Dahm, W. J. A., Frieler, C. E., and Tryggvason, G., "Vortex Structure and Dynamics in the Near Field of a Coaxial Jet," *Journal of Fluid Mechanics*, Vol. 241, 1992, pp. 371–402.

[18]Tang, S. K., and Ko, N. W. M., "Experimental Investigation of the Structure Interaction in an Excited Coaxial Jet," *Experimental Thermal and Fluid Science*, Vol. 8, No. 3, 1994, pp. 214–229.

[19]Wicker, R. B., and Eaton, J. K., "Near Field of a Coaxial Jet With and Without Axial Excitation," *AIAA Journal*, Vol. 32, No. 3, 1994, pp. 542–546.

[20]Rehab, H., Villermaux, E., and Hopfinger, E. J., "Flow Regimes of Large-Velocity-Ratio Coaxial Jets," *Journal of Fluid Mechanics*, Vol. 345, 1997, pp. 357–381.

[21]Ko, N. W. M., and Chan, W. T., "The Inner Region of Annular Jets," *Journal of Fluid Mechanics*, Vol. 93, Pt. 3, 1979, pp. 549–584.

[22]Ko, N. W. M., and Lam, K. M., "Flow Structures of a Basic Annular Jet," *AIAA Journal*, Vol. 23, No. 8, 1985, pp. 1185–1190.

[23]Lam, K. M., and Ko, N. W. M., "Investigation of Flow Structures of a Basic Annular Jet," *AIAA Journal*, Vol. 24, No. 9, 1986, pp. 1488–1493.

[24]Wlezian, R. W., and Kibens, V., "Noise-Related Shear-Layer Dynamics in Annular Jets," *AIAA Journal*, Vol. 23, No. 5, 1985, pp. 715–722.

[25]Leung, R. C. K., Chu, W. F., Tang, S. K., and Ko, N. W. M., "Control of Vortex Pairing Sound," *AIAA Journal*, Vol. 35, No. 5, 1997, pp. 802–809.

[26]Tang, S. K., and Ko, N. W. M., "Effects of a Background Axisymmetric Potential Flow on Vortex Ring Pairing Sound," *Journal of the Acoustical Society of America*, Vol. 104, No. 6, 1998, pp. 3273–3281.

[27]Weidman, P. D., and Riley, N., "Vortex Ring Pairs: Numerical Simulation and Experiment," *Journal of Fluid Mechanics*, Vol. 257, 1993, pp. 311–337.

[28]Saffman, P. G., *Vortex Dynamics*, Cambridge Univ. Press, Cambridge, England, U.K., 1995, pp. 209–229.

[29]Tang, S. K., "The Aeroacoustics of Free Shear Layers and Vortex Interactions," Ph.D. Dissertation, Dept. of Mechanical Engineering, Univ. of Hong Kong, Hong Kong, PRC, Sept. 1992.

[30]Morse, P. M., and Feshbach, H., *Methods of Theoretical Physics*, McGraw–Hill, New York, 1953, pp. 1252–1308.

[31]Olsen, W., and Friedman, R., "Jet Noise from Coaxial Nozzles over a Wide Range of Geometric and Flow Parameters," NASA TMX-71503, 1974.

J. C. Hermanson
Associate Editor